RESEARCH ARTICLE

NMR IN BIOMEDICINE **WILEY**

Tracking gonadal development in fish: An in vivo MRI study on polar cod, *Boreogadus saida* (Lepechin, 1774)

Nicole Vogt[1] | Felizitas C. Wermter[2] | Jasmine Nahrgang[3] |
Daniela Storch[1] | Christian Bock[1]

[1]Integrative Ecophysiology, Alfred-Wegener-Institute Helmholtz Centre for Polar and Marine Research, Bremerhaven, Germany

[2]Department of Chemistry, in-vivo-MR group, University Bremen, Bremen, Germany

[3]Department of Arctic and Marine Biology, UiT The Arctic University of Norway, Tromsø, Norway

Correspondence
Christian Bock, Integrative Ecophysiology, Alfred-Wegener-Institute Helmholtz Centre for Polar and Marine Research, Am Handelshafen 12, 27570 Bremerhaven, Germany.
Email: christian.bock@awi.de

Funding information
Alfred Wegener Institute Helmholtz Centre for Polar and Marine Research

Abstract

Magnetic resonance imaging (MRI) was applied to determine the sex of polar cod (*Boreogadus saida* Lepechin, 1774) (Actinopterygii: Gadidae) and to follow the gonadal development in individual animals over time. Individual unanaesthetised fish were transferred to a measurement chamber inside a preclinical 9.4 T MRI scanner and continuously perfused with aerated seawater. A screening procedure at an average of 3.5 h, consisting of a set of MRI scans of different orientations, was repeated every 4 weeks on the same set of reproducing *B. saida* ($n = 10$) with a body length of about 20 cm. Adapted multi-slice flow-compensated fast low-angle shot (FcFLASH) and rapid acquisition with relaxation enhancement (RARE) protocols with an in-plane resolution of 313 μm and an acquisition time of 2.5 min were used to visualise the morphology of various organs, including the gonads within the field of view (FOV). The MR images provided high resolution, enabling specific sex determination, calculation of gonad volumes, and determination of oocyte sizes. Gonad maturation was followed over 4 months from November 2021 until shortly before spawning in February 2022. The gonad volume increased by 2.3–25.5% for males and by 11.5–760.7% for females during the observation period. From October to February, the oocyte diameter increased from 427 μm ($n = 1$) to 1346 ± 27 μm ($n = 4$). Interestingly, individual oocytes showed changes in MR contrast over time that can be attributed to the morphological development of the oocytes. The results fit well with previous literature data from classical invasive studies. The presented approach has great potential for various ecophysiological applications such as monitoring natural or delayed development of internal organs or sex determination under different environmental conditions.

KEYWORDS
Arctic cod, gonad maturation, magnetic resonance, non-invasive

1 | INTRODUCTION

The study of the sensitivity of marine species to climate change and associated stressors is of great importance in providing information on climate-induced changes in marine ecosystems. In vivo experimental studies are often interested in monitoring physiological responses over time. A typical example is the evaluation of gonad maturation of reproducing individuals. A critical aspect involves evaluating pivotal life stages, such as the gonadal maturation of reproducing individuals and comprehending the physiological response during such crucial periods. Such studies typically require the sacrifice of large numbers of animals for sex determination (e.g. previous studies[1–5]), alongside histological assessments of their maturity status and gonad development under natural conditions or additional environmental stressors such as rising temperatures or crude oil exposure (e.g. Bender et al. and Strople et al.[6,7]). Additionally, such studies often suffer from imbalanced sex-ratios, prompting compensatory measures such as expanding the sample size to account for the disparity.[8] Adhering to the 3 R principle (replace, reduce and refine),[9,10] the goal is to minimise the number of experimental animals while refining experiments to facilitate measurements of sensitive life phases, such as gonadal maturation in marine organisms.

In addition to classical destructive methods, there are a few non-invasive 3D imaging techniques such as computed tomography (CT), ultrasound and magnetic resonance imaging (MRI) to study the development of reproductive organs (reviewed in Clear et al.[11]). Repeated examinations of the reproductive organs on the same individuals by CT might cause damage to the reproductive organs or developing germ cells. Ultrasound has been demonstrated to be a rapid and useful tool for sexing and estimating gonad volume in anaesthetised fish (e.g. other works[12–14]) but is limited in terms of resolution and contrast. MRI is a widely used application in clinical and preclinical studies. It has also been suggested for anatomical imaging in zoology for a broad range of taxa.[15] Blackband and Stoskopf[16] were the first to use in vivo MRI on marine and anaesthetised organisms, and Bock et al.[17] refined measuring procedures to apply MRI on non-anaesthetised fish. In recent years, studies applying MRI on aquatic organisms have become more frequent and have been successfully estimating adipose tissue,[18] lipid distribution ex vivo in brown trout (*Salmo trutta* Linnaeus, 1758)[19] and studying neurological diseases in the brain of zebrafish (*Danio rerio* Hamilton, 1822).[20–22] Pan et al.[23] successfully applied MR imaging techniques using a clinical MR scanner to study ovarian maturation on an anaesthetised freshwater fish species, the cyprinid *Rhinogobio ventralis* (Sauvage & Dabry de Thiersant, 1874).

The major advantage of the MR approach is the possible combination of different MR imaging techniques to study the physiological response of aquatic organisms more comprehensively (reviewed in Kaneko et al. and van der Linden[24,25]). T1- and T2-weighted MR techniques allow for morphological observations, for example the separation of organs or observations for dietary status such as fat/lipid content,[26] and flow-weighted MRI techniques can be used to study the circulatory performance of marine organisms, measuring the blood flow and creating an angiography of the cardiovascular system.[27] Thus, the combination of different MRI techniques can provide a more holistic picture of an organism's physiological response to, for example changing temperatures.

Besides its direct impact on the metabolism of individual organisms, ocean warming will lead to a decline in important organismal performance parameters,[28] such as growth, foraging and reproduction, which are essential for a species' survival in its ecosystem.[29,30] The polar regions are particularly threatened by climate change leading to the question of how highly adapted polar organisms can cope with the rapid changes. Therefore, we used an Arctic fish as a model organism. Polar cod (*Boreogadus saida* Lepechin, 1774) has a circumarctic distribution[31] and is considered the most abundant forage fish species linking lower and higher trophic levels in the Arctic food web.[32–34] *B. saida* is an iteroparous spawner (species with multiple reproductive cycles throughout their lifespan)[1,35,36] and reaches maturity at an age of 2–3 years, males and females, respectively.[37] Gonad maturation in both sexes starts around August and spawning occurs from November to March with the main spawning season in January and February (reviewed in Hop and Gjøsæter[38]). Eggs are buoyant, transparent and the largest among the Gadidae.[39,40]

The aim of this study was to develop a non-invasive longitudinal screening procedure for gonad monitoring by adapting standard MRI protocols to follow the gonad maturation in individual polar cod of both sexes, to calculate gonad volume and to determine oocyte size. The method was validated and compared by sacrificing the fish at the end of the experiment. Gonadosomatic index (GSI) was determined based on gonad weight and gonad volume at the endpoint of the experiment. And thus, demonstrating that the maturation stage of an individual can be determined without dissecting it and reducing the overall number of animals needed for long-term experiments on reproducing polar cod.

2 | MATERIAL AND METHODS

2.1 | Animals

Polar cod were caught using a pelagic fish trawl combined with a fish-lift on the Heincke Cruise HE560 in Kongsfjorden at a depth of 200–300 m around Svalbard, Norway in August 2020. The animals were transported back to the aquarium at the Alfred-Wegener-Institute in Bremerhaven, Germany. *B. saida* were held in shoals sorted by size to avoid cannibalism in 450-L tanks using a recirculating water system with natural seawater at 0.0–0.3°C and 32- to 33-ppt salinity until the start of the experiments in September 2021. Animals were fed twice a week with frozen squid (Erdmann, Ritterhude, Germany). For individual recognition, animals were tagged at the beginning of the experiment with VI Alpha Tags

(Northwest Marine Technology, Inc., Anacortes, Washington, United States) using 125 mg/L of MS-222 (ethyl-3-aminobenzoate-methansulfonate, Sigma-Aldrich, Saint Louis, Missouri, United States) for anaesthesia. The tagging procedure lasted no longer than 20 min. All animals recovered shortly after anaesthesia without any constraints.

Experiments in this study were performed according to German animal welfare regulations and approved within the 'KliPo-Fisch' project (Freie Hansestadt Bremen, reference number 160; 500-427-103-7/2018-1-5).

2.2 | Monitoring of gonad development

Ten *B. saida*, five males (M1–M5) and five females (F1–F5), with a length of 20 ± 1 cm and a weight of 40.8 ± 6.3 g (only recorded at the end of the study to reduce handling) were used in this study. The experiment was performed from September 2021 until the end of February 2022. The monitoring period of gonadal development started on 15.09.2021 (hereafter referred to as Day 1) the day when the first fish was scanned. During September and October 2021, the applied MRI protocols were modified for *B. saida* to achieve reliable results. Thereafter, the time in the scanner per fish could be reduced to 3 h. However, only partial MR imaging sets could be acquired in October 2021 (Table 1), and reliable quantification of the gonad volume at the onset of gonad maturation was not possible. Comparable gonad volume determinations using standardised MRI sets started in November 2021. The gonad volume of males and females was quantified between November 2021 (from Day 69 of the monitoring time onwards) and February 2022. The MRI data of November and December 2021 (monitoring Days 69–91) will be considered as one time point during the analysis and referred to as Nov 21. One individual was measured at a time; therefore, individuals were investigated on different days leading to an observation period instead of a single time point for each month. The exact monitoring time points for each individual are summarised in Table 1.

One female (F4) spawned in the holding tank between January 2022 and February 2022. The exact time point could not be determined. In addition, three females spawned inside the MR scanner after the standardised MRI protocols were completed, so that we had the opportunity to take images immediately before and after spawning. Within 24 h after the last MRI measurement, polar cod were sacrificed using an overdose of MS-222 (500 mg/L). Ecological relevant parameters such as total length (TL) (cm) (length including caudal fin), standard length (SL) (cm) (length from head to last vertebra excluding caudal fin), total weight (TW) (g), and gonad weight (GW) (g) were recorded, and the GSI was determined according to measured weights during dissection according to Equation 1:

$$GSI = \frac{GW}{TW} * 100 \, (\%).$$ (1)

Furthermore, to calculate the GSI prior to dissection, a gonad volume-based GSI was determined according to Equation 2:

$$GSI_{VG} = \frac{VG}{TW - GW + VG} * 100 \, (\%),$$ (2)

with TW corrected for the gonad weight at dissection and replaced by the MRI-based gonadal volume (VG). The GSI $_{VG}$ was calculated to obtain an estimation for the females (F2, F3, F5) that spawned inside the MRI scanner. The TW was recorded at dissection; hence, to estimate the GSI prior to spawning, the TW had to be corrected due to the weight lost at spawning. The gonad weight was replaced by gonad volume, assuming a weight:volume ratio of 1 based on the linear correlation of gonad weight and gonad volume found in this study. To validate this approach, the GSI and GSI $_{VG}$ of all polar cod were compared (see Section 3.2).

TABLE 1 Observation period for gonadal development of each polar cod. The monitoring Day 1 took place on 15.09.21. After adjusting the protocols, images were acquired from monitoring Day 41 to the final Day 166 on 27.02.22, n.a.: data not available, M: male, F: female.

Month/individuals	Monitoring time (d)									
	M1	M2	M3	M4	M5	F1	F2	F3	F4	F5
Oct 21	41	n.a.	n.a.	n.a.	n.a.	36	n.a.	n.a.	n.a.	n.a.
Nov 21	69	71	72			70				
Dec 21				85	90		79	84	86	91
Jan 22	126	122	120	119	129	121	121	126	120	127
Feb 22	160	162	148	156	166	158	150	154	164	152

2.3 | Experimental design

A 350-mL Perspex flow-through chamber (24 cm × 4 cm × 4.5 cm) containing a single unanaesthetised and unrestrained fish was placed in the centre of the MR scanner and was continuously perfused with aerated seawater (Figure 1). The chamber was connected to an in-house built circulating system with a 50-L water reservoir outside of the MR scanner room, which allowed the regulation of the seawater temperature to 0.5 ± 0.5°C (for details, see Bock et al. and Wermter et al.[17,41]). The water flow was set to 500 mL/min. The seawater was changed with pre-cooled seawater after 4 animals were scanned. After being transferred to the Perspex chamber, the fish calmed down after a couple of minutes and were left for max. 15 min prior to measurements. The time for individual fish in the MR scanner was at an average of 3.5 h to complete all MRI scans. From November onwards, the time in the MR scanner was reduced to 3 h after finalising imaging parameters. After a set of MRI measurements, the animal was immediately transferred back to the holding tank. This procedure was repeated every 4 weeks for each fish.

2.4 | MRI protocol

In vivo MRI measurements were performed using a 9.4 T animal scanner with a 30-cm horizontal bore (BioSpec 94/30 Avance III, Bruker BioSpin, Ettlingen, Germany) and a BGA-12S gradient system combined with a 1H quadrature coil with an inner diameter of 86 mm. All images were recorded using ParaVision software (V.6.0.1, Bruker BioSpin MRI, Germany) (see also [41]). Two standard methods for anatomical imaging were tested. Different issues for both flow-compensated fast low-angle shot (FcFLASH) and rapid acquisition with relaxation enhancement (RARE) techniques were encountered. The FcFLASH method produced clear anatomical images, but male gonads could not be detected showing lower contrasting gonads compared with surrounding tissue. The RARE method was very sensitive to movement artefacts and the surrounding seawater flow. The problems of moving individuals in the chamber and water flow were overcome by reducing the acquisition time of sagittal FcFLASH, sagittal and coronal RARE images and axial RARE images. Finally, standardised parameters for each method were used to compare both methods (Table 2). The T1 and T2 values of polar cod gonads in November ranged from 1209.12 to 1229.33 ms and from 57.84 to 99.81 ms, respectively. Therefore, the selected parameters were a compromise between acquisition time and determined T1 and T2 values. RARE images were used for the final MR analysis of gonad volume of males and females and the measure of oocyte diameter.

Fish were positioned in the centre of the coil using localiser scans in all three directions (FLASH, flip angle = 30°, echo time [TE] = 4.0 ms, repetition time [TR] = 100.0 ms, 128 × 128 pixels, field of view [FOV] = 80 mm², slice thickness = 2 mm, 3 slices). Anatomical MRI of *B. saida* was recorded using FcFLASH, and gonad anatomy of both sexes was recorded using sagittal and coronal 2D-multi-slice RARE images (see Table 2). Sagittal slice packages were positioned posterior to the gills to avoid movement artefacts from ventilation and to cover the whole length of the fish (Figure 1B); 1–3 saturation pulses (sech pulse, length = 4.05 ms, bandwidth = 5000 Hz, flip angle = 90°, sharpness = 3, module duration = 4.975 ms) were used for FOV saturation, which were positioned along the body, reducing movement artefacts from surrounding sea water. In addition, we performed axial-orientated RARE images with a higher resolution (150 × 150 µm) to resolve changes within the gonads, for
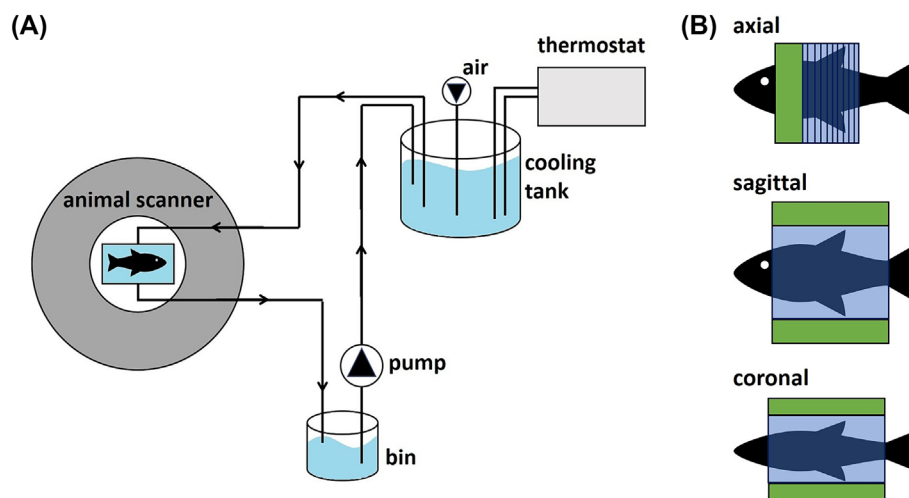

FIGURE 1 Magnetic resonance imaging (MRI) experimental setup and schematic of field of views (FOV), (A) in vivo set up with recirculating seawater system, flow-through chamber and cooling tank (adjusted after [41]), (B) position of slice packages using different FOVs, blue box = FOV, green box = saturation slices.

TABLE 2 Acquisition parameters for MR imaging of *B. saida* with gonads in flowing seawater at 500 mL per min. Two RARE scans with different resolutions were required for gonads and oocytes.

Applications	Anatomy	Anatomy/ gonad volume	Oocyte diameter
Method	FcFLASH	RARE	RARE
TE (ms)	4.63	60.77	68.91
TR (ms)	250.45–363.15	3064.706–4091.418	2000 and 4000[a]
Averages	2	4	4
Excitation angle (°)	45	90	90
Refocusing angle (°)	-	180	180
Bandwidth (Hz)	50,000	50,000	50,000
RARE factor	-	16	16
Matrix size (pixels)	256 × 175 sagittal	256 × 175 sagittal, coronal	300 × 300 axial
FOV (mm x mm)	80 × 54.69	80 × 54.69	45 × 45
FOV saturation (mm)	n.a.	1 × sagittal 10 1 × coronal 10	1 × axial 20
Resolution (μm)	313 × 313	313 × 313	150 × 150
Slice gap (mm)	0.1	0.1	0
Slices (No.)	18–29	18–29	10
Slice thickness (mm)	1	1	1
Acquisition time (min:s:ms)	01:36:422–02:07:102	01:59:398–02:43:656	02:24:000

Abbreviations: FcFLASH, flow-compensated fast low-angle shot; FOV, field of view; RARE, rapid acquisition with relaxation enhancement; TE, echo time; TR, repetition time.
[a]TR 4000 ms only used in October 2021.

example oocyte development. The FOV of axial RARE was always positioned close to the second pectoral fin to obtain comparable data over time.

2.5 | Image processing

To calculate the gonad volume for males and females, sagittal RARE images were imported to Fiji (Fiji is Just ImageJ) Version 2.3.0/1.53t, and regions of interest (ROIs) were manually drawn around the gonadal tissue in each slice of the sagittal 2D multi-slice RARE stack. The gonad area in each slice was multiplied by the slice thickness of 1 mm to obtain the volume (V_n) in each slice. Afterwards, all volumes were summed up and corrected for the slice gap between two slices according to Equation 3. For each individual and time point, 3–4 technical replicates were analysed, and mean and standard deviation were calculated. Gonad volume (VG) in cm^3 including a slice gap of 0.1 mm between slices was calculated according to the following equation:

$$VG = \sum_{k=1}^{n} \frac{(V_1 * 1.05 + V_2 * 1.1 + V_{n-1} * 1.1 + V_n * 1.05)}{1000} \; (cm^3), \tag{3}$$

with V_n = volume of each slice mm^3 (area [ROI] multiplied by slice thickness = 1 mm), n = number of slices in MRI stack. The first and last slices have only one neighbouring slice and therefore share only one slice gap multiplied by 1.05. Coronal RARE images were additionally analysed for male M1 and M2 because the sagittal views did not completely cover the entire gonads. Because coronal and sagittal RARE images were analysed for M1 and M2, the imaging stacks with the greatest gonad coverage were used for volume determination.

The developing oocyte or egg in the female gonad is hereafter referred to as oocyte because we are only able to determine the size but not the exact maturation stage of the egg cells. The oocyte size was directly measured in axial-orientated RARE images using ParaVison (V.6.0.1, Bruker BioSpin MRI, Germany). The resolution of our axial RARE images was limited to an in-plane resolution of 150 μm, oocytes could only be measured after reaching a size greater than 200 μm. Ten large, clearly visible oocytes in the same image were randomly selected, and size was determined by taking the diameter. For each female, three images of a different image stack per time point were analysed, and mean oocyte size (μm) and standard deviation were calculated. Just before spawning in February 2022, we estimated the total number of oocytes per female by

dividing the gonad volume (converted to mm^3) by the oocyte volume (mm^3), assuming no interspace of connective tissue between oocytes at this point of maturation and a spherical shape of the oocytes.

2.6 | Statistics

Females F1 and F4 that spawned partially in February were identified as outliers for gonad volume and oocyte volume: gonad volume ratio. Outliers were tested for statistical significance via Cook's distance and excluded from further calculations. Data were tested for normal distribution using visual inspection (by QQ plots) and Shapiro–Wilk tests. Simple linear regression was performed for the gonad weight: gonad volume correlation and the oocyte volume: gonad volume correlation. Additionally, the Pearson correlation coefficient was calculated. Linear mixed effect models (LME) fitted by restricted maximum likelihood (REML) were performed for repeated measures such as gonad volume and oocyte diameter over time. A local polynomial regression fit (loess) was applied to visualise oocyte development. The chosen level of significance for all tests was alpha = 0.05. All statistical analyses were performed in R studio (V4. 3. 1)[42–45] using 'dplyr', 'ggmisc', 'ggplot2', 'ggpubr', 'nlme', 'openxlsx', 'RColorBrewer' and 'rstatix' packages.

3 | RESULTS

3.1 | MRI methods: FcFLASH versus RARE

Figure 2 shows the comparison between sagittal multi-slice FcFLASH and RARE image stacks for anatomical studies of male and female gonads. Both imaging methods show clear differences in brightness and contrast (Figure 2). The FcFLASH images are characterised by a low contrast and organs such as the swim bladder (sw), urine bladder (u) or vertebrae (v) are clearly visible (Figure 2A,D). In contrast, the RARE images generally appeared darker (Figure 2B,C,E,F) with a clear separation of the stomach (s). Interestingly, the surrounding seawater did not appear uniform but in varying signal intensity in the RARE images compared with FcFLASH images.

Both methods can be used to distinguish between males and females of *B. saida*. The testes were identified as a light grey mass with small inlets (marked in light blue in Figure 2C). The ovaries were identified as a dark grey mass with small roundish structures (oocyte) (marked in dark blue in Figure 2F). Female gonads could be distinguished from surrounding tissue in FcFLASH images, whereas the contrast of male gonads were very similar to the surrounding tissues (Figure 2A,D). Furthermore, FcFLASH images showed susceptibility artefacts (sa) close to the swim bladder
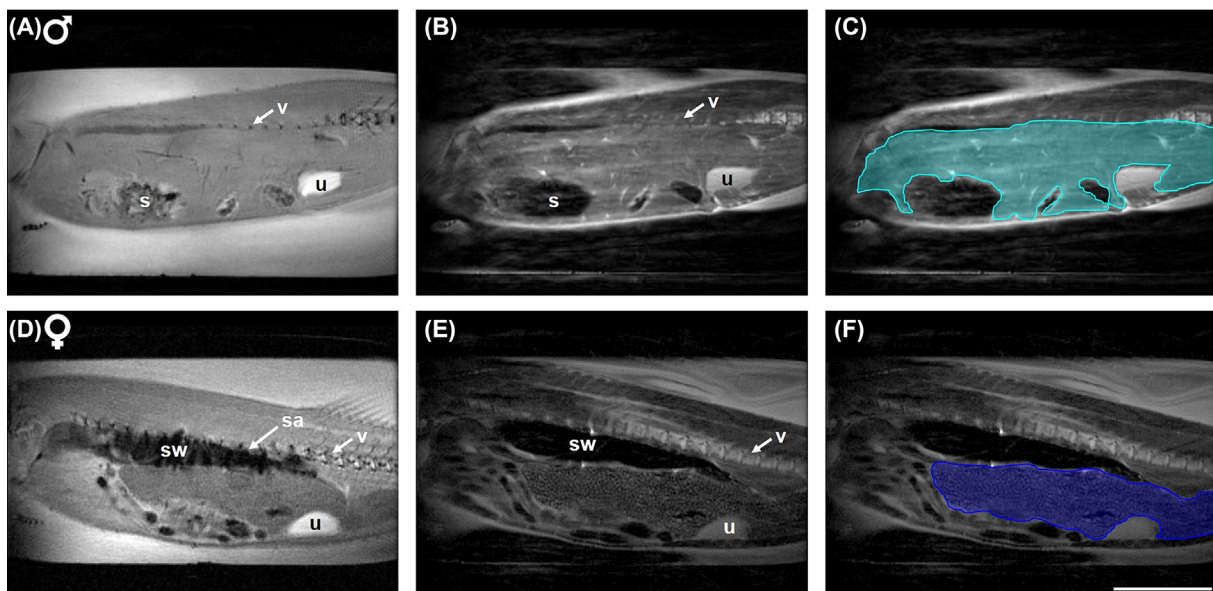

FIGURE 2 Magnetic resonance imaging (MRI) comparison between flow-compensated fast low-angle shot (FcFLASH) and rapid acquisition with relaxation enhancement (RARE). Sagittal 2D multi-slice images of the gonads of one male (A–C) and one female (D–F) are displayed as FcFLASH (A,D) and RARE (B,C, E,F). Gonads were coloured for better identification (for acquisition parameters, see Table 2). sa = susceptibility artefacts, sw = swim bladder, s = stomach, u = urine bladder, v = vertebrae. The scale bar corresponds to 2 cm. Images were taken in November 2021.

(Figure 2D), which could influence the calculated gonad volume given the fact that the gonads are right underneath the swim bladder. In comparison, the RARE method produced images where male and female gonads could be clearly distinguished from surrounding organs. Therefore, RARE images were used to monitor gonadal development and determine gonad volume.

3.2 | MRI volume as proxy for gonad weight—Method validation

In February, the measured gonad weight and MRI-based volume of testes and ovaries revealed a positive correlation with a Pearson correlation coefficient of 0.80 for males and 0.99 for females. The gonad volume increased with increasing weight with a slope near 1 (Figure 3). The observed correlation was only statistically significant in ovaries. Pearson's r-squared of the weight: volume correlation of the testis was 0.64 compared with 0.99 in ovaries (Figure 3).

The gonad weight and volume were used to calculate the GSI. The GSI based on gonad weight was comparable with the GSI $_{VG}$ based on MRI-based gonad volume as shown in Table 3. For the three females (F2, F3 and F5) that spawned inside the MR scanner pre-spawning GSI $_{VG}$ and post-spawning GSI $_{VG}$ are displayed. For males, the volume-based GSI $_{VG}$ was consistently larger than the weight-based GSI. For females, the volume-based GSI $_{VG}$ coincided well with the weight-based GSI.
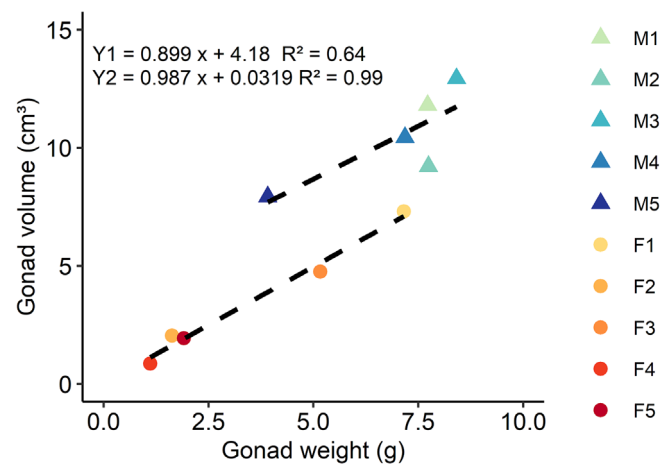

FIGURE 3 Correlation of gonad weight and magnetic resonance imaging (MRI)-based gonad volume of males ($n = 5$, triangles) and females ($n = 5$, circles) in February 2022. The regression analysis (dashed lines) depicting the correlation between calculated gonad volume and gonad weight is Y1 = 0.899x + 4.18 for males ($R^2 = 0.64$, $p > 0.05$) and Y2 = 0.987x + 0.0319 for females ($R^2 = 0.99$, $p < 0.05$). *Note*: The presented gonad weight and gonad volume of females F2, F3 and F5 were determined after spawning inside the MR scanner.

TABLE 3 GSI of *B. saida* in February 2022, GSI = classical approach, calculation based on weight in g determined after dissection (Equation 1), GSI $_{VG}$ = calculation based on MRI-based gonad volume (Equation 2) and GSI $_{VG}$ = calculation based on MRI-based gonad volume post-spawning (Equation 2).

Individuals	Gender	GSI (%)	GSI $_{VG}$ (%)	GSI $_{VG}$ (%) post-spawning
M1	Male	14.8	20.9	n.a.
M2	Male	16.2	18.7	n.a.
M3	Male	14.7	20.9	n.a.
M4	Male	15.2	20.7	n.a.
M5	Male	11.0	20.1	n.a.
F1	Female	12.1	12.4	n.a.
F2	Female	3.8	46.3	4.8
F3	Female	12.6	45.6	11.6
F4	Female	3.1	2.4	n.a.
F5	Female	4.5	47.8	4.6

Abbreviations: GSI, gonadosomatic index; MRI, magnetic resonance imaging; VG, gonadal volume.

3.3 | Male gonad development

A representative time series of axial RARE images of one male *B. saida* (M1) shows the light grey testes underneath the swim bladder and liver (Figure 4). Over the monitoring period of 4 months, only small changes in image contrast of male gonads could be observed. From Day 41 (Oct 21, *n* = 1) to Days 119–126 (Jan 22, Figure 4A–C), the testes showed a homogenous contrast, at Days 148–166 (Feb 22), shortly before spawning the gonads showed a more heterogenous pattern with areas of higher and lower signal intensity (Figure 4D). This change was not uniform over the whole gonad tissue but limited to certain areas in two males (M1 and M3). In the other three males (M2, M4 and M5), the change to very light grey was observed in the entire gonad tissue.

The overall MRI-based volume of male gonads increased slightly over time. Individual variation of gonad volume in males is leading to a rather inconsistent picture (Figure 5), as reflected by the running mean (dashed line). The mean gonad volume was 9.7 ± 1.9 cm^3 at Days 69–90 (Nov 21) and increased slightly to 10.5 ± 1.8 cm^3 at Days 148–166 (Feb 22). Two males (M1 and M2) showed an intermitted drop in gonad volume in January, and M2 did not reach the same or higher gonad volume on day 162 compared with Day 71. Between November 2021 and February 2022, the increase in gonadal volume in individual males varied widely between 2.3% and 25.5% except for M2, which showed a decrease of 15.8% from November to February, but an increase of 9.5% from January to February. The observed trends were not significant. In February 2022, the average GSI $_{VG}$ of males (*n* = 5) was 20.3 ± 1.8% using MRI-based gonadal volume.

3.4 | Female gonad and oocyte development

In contrast to testes, female gonads underwent a broad change in contrast and volume from October 2021 to February 2022. In the axial view, the ovary was visible as two round organs located ventral to the swim bladder and liver (Figure 6). From Day 36 (Oct 21) to 121 (Jan 22), single
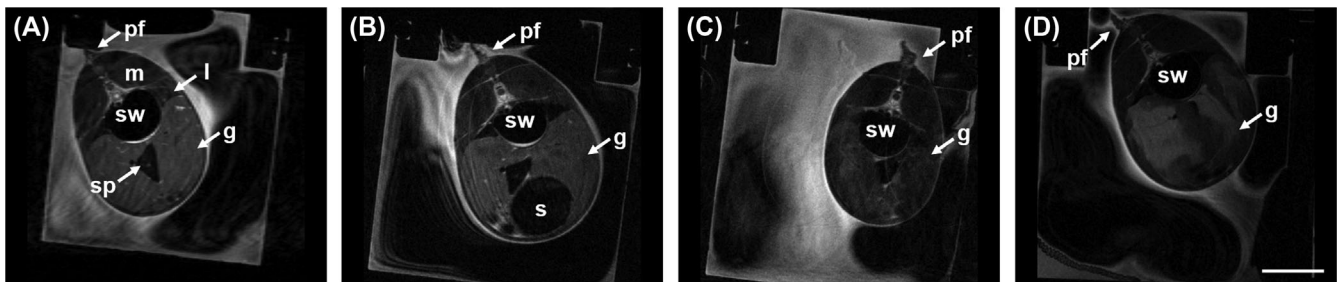

FIGURE 4 Time series of gonadal development of male *Boreogadus saida* (M1) taken on monitoring days (A) 41 (Oct 21), (B) 71 (Nov 21), (C) 126 (Jan 22) and (D) 162 (Feb 22). Axial, cross-sectional rapid acquisition with relaxation enhancement (RARE) images, FOV = 45 × 45 mm^2, 300 × 300 pixels, slice thickness = 1 mm. Repetition time (TR) was for images (A) 4000 ms, (B–D) 2000 ms. g = gonad, l = liver, m = muscle, pf = second pectoral fin, sp = spleen and sw = swim bladder, s = stomach. The scale bar corresponds to 1 cm.
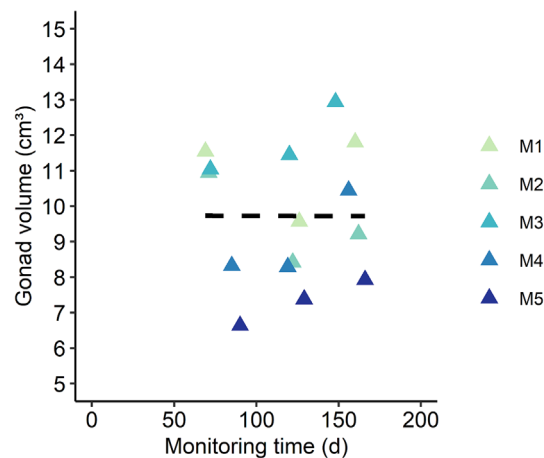

FIGURE 5 Gonad volume of male *Boreogadus saida* (*n* = 5) based on sagittal rapid acquisition with relaxation enhancement (RARE) images from November 2021 (Days 69–90) to February 2022 (Day 148–166), dashed line = rolling mean per monitoring period (*n* = 5). No significant changes over time (linear mixed effect models [LME], *p* > 0.05).
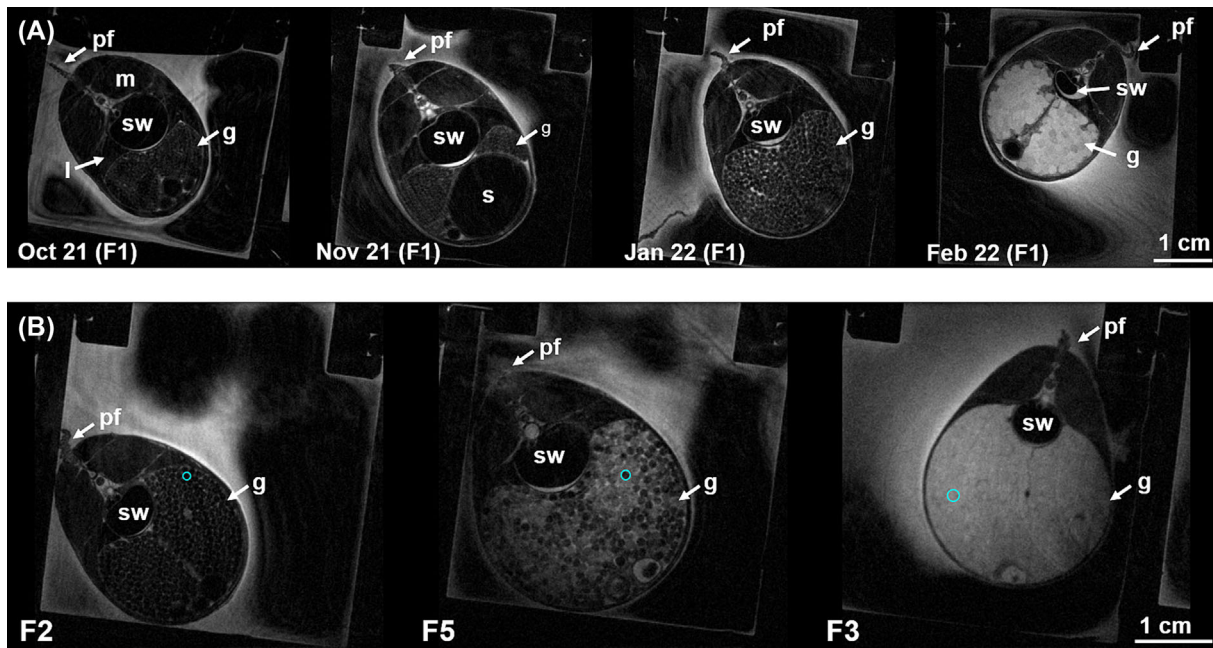
FIGURE 6 (A) Time series of the gonadal development of one female *Boreogadus saida* (F1) taken on monitoring days 36 (Oct 21), 70 (Nov 21), 121 (Jan 22) and 158 (Feb 22); (B) female gonads in January 2022 with different maturation stages of oocytes, F2 monitoring Day 121, F5 monitoring Day 127, F3 monitoring Day 126.; the less mature gonads of F2 show a dark contrast and oocyte diameters of 814 ± 7 μm; F5 has gonads with inhomogeneous contrast from dark grey to a light grey and oocyte diameter of 928 ± 24 μm, and F3 shows advanced gonads with very high contrast and oocyte diameter of 1164 ± 15 μm. Axial, cross-sectional rapid acquisition with relaxation enhancement (RARE) images, field of view (FOV) = 45 × 45 mm^2, 300 × 300 pixels, slice thickness = 1 mm. TR = 2000 ms (except image Oct 2021: repetition time [TR] = 4000 ms). g = gonad, l = liver, m = muscle, pf = second pectoral fin, sp = spleen and sw = swim bladder, s = stomach; single oocyte marked with a light blue circle, scale bar corresponds to 1 cm.

oocytes were clearly visible and showed a dark contrast in the early developmental phase (Figure 6A). At Days 120–127, gonad volume and oocyte diameter increased notably. At Days 152–164, shortly before spawning, oocytes showed a high contrast. Further, we found one female (F5), which displayed an intermediate state of gonad maturation, where the contrast of some oocytes already changed from a very dark to a lighter grey in January 2022 (Days 120–127) (Figure 6B).

The gonadal development was monitored from Day 1 to Day 164; at Day 70, we were able to estimate the gonad volume of female *B. saida* for the first time. The gonad volume increased significantly between November 2021 and January 2022 and from January 2022 to February 2022. The mean MRI-based gonad volume increased from 5.4 ± 1.3 cm^3 at Days 70–91 to 22.1 ± 16.1 cm^3 at Days 150–164. Between Days 120 and 127, females showed high variability with a mean gonad volume of 13.1 ± 5.0 cm^3 (ranging from 6.3 cm^3 to 18.5 cm^3) indicating a rapid change in gonadal development (Figure 7A). The gonad volume increased by 320–760% from Days 79–91 to Days 150–154 for F2, F3 and F5 resulting in a GSI $_{VG}$ of 46.5 ± 0.9% of pre-spawning females. For two individuals, the gonad volume increased only until January 2022 (Days 120 and 121) by 58% and 131% (for F4 and F1) and decreased significantly compared with the other females at Days 158 and 164, respectively. This may have been related to the later measuring point or a missed spawning event in the holding tank. This is also reflected in a lower GSI $_{VG}$ of 12.4% for F1 and 2.4% for F4 in February 2022.

Oocytes showed a sigmoid growth pattern illustrated by the running mean in Figure 7B. On Day 36, we were able to measure the oocyte diameter for the first time (Figure 7B). The oocyte diameter increased significantly from 427 μm at Day 36 (only one female was measured, $n = 1$) to 1346 ± 24 μm at Days 150–158 ($n = 4$). Between Days 70 and 91, females showed a similar gonad development stage with a mean oocyte diameter of 562 ± 11 μm ($n = 5$). The large variability in gonadal volume between Days 120 and 127 was also reflected in a higher standard deviation of the mean oocyte diameter at this time point, 869 ± 166 μm ($n = 5$). At the end of the observation period, all observed females reached a similar oocyte diameter of about 1346 ± 24 μm ($n = 4$), except female F4, where no oocyte diameter could be measured due to a previous spawning event. The estimated total number of oocytes per female was between 16,693 and 29,735 (mean 21,364 ± 9425) in February 2022. The development of oocyte size correlated positively with gonad volume (Figure 7C, R^2 of 0.93). The gonad volume increased significantly with increasing oocyte size with a slope of 22.76 and a Pearson correlation coefficient of 0.965.

In February 2022, three females spawned inside the MR scanner after the data for gonad volume, and oocyte diameter had been recorded. Figure 8 shows the cross-section of one female immediately before spawning and after the release of all oocytes. A massive volume loss was
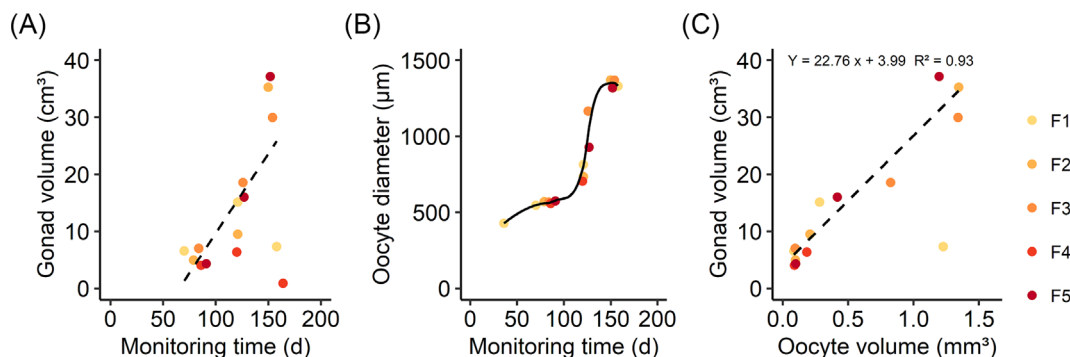
FIGURE 7 (A) Gonad volume and (B) oocyte diameter of *Boreogadus saida* females as a function of time and (C) the correlation of gonad volume over oocyte volume. (A) Gonad volume (cm^3) is based on sagittal rapid acquisition with relaxation enhancement (RARE) images taken in November 2021 (Days 70–91), January 2022 (Days 120–127) and February 2022 (Days 150–164. The dashed line represents the running mean ($n = 5$: F1–F5, F4 at Day 165 as outlier excluded). Significant increase between observation periods (linear mixed effect models [LME], $p < 0.05$). *Note*: F1 and F4 (partially) spawned in the holding tank before the last monitoring time in February leading to a drastic decrease in gonad volume. (B) Oocytes were measured between Days 36 and 158 of the monitoring phase (Oct 21–Feb 22), $n = 5$, at Day 36: $n = 1$, at Days 150–164: $n = 4$. The solid line represents the 'loess' smoothing fit. Significant increase between observation periods (LME, $p < 0.05$). Standard deviation is too small to be displayed. (C) The dashed line represents the linear regression $Y = 22.76 x + 3.99$ ($R^2 = 0.93$, $p < 0.05$), excluding an outlier value (F1 [$1.2 mm^3$/$7.3 cm^3$]).
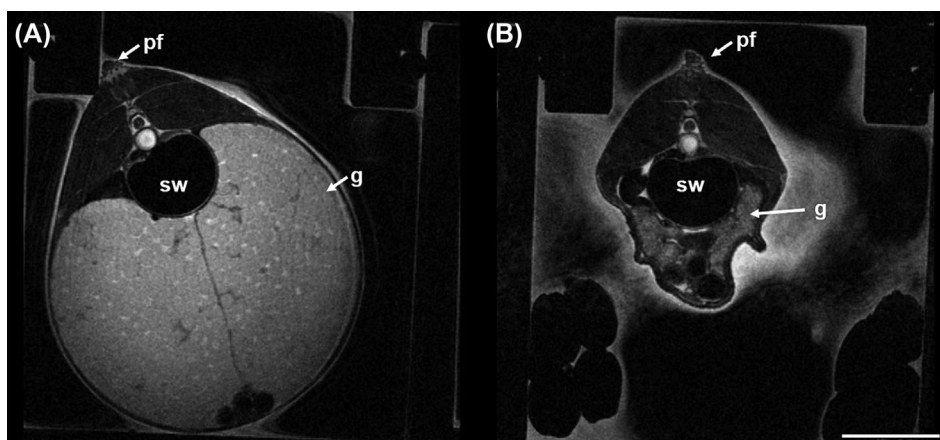

FIGURE 8 Female gonad (F5) in February 2022 before and after spawning in the magnetic resonance (MR) scanner, monitoring Day 152; (A) female before spawning at 4:13 pm, (B) female after spawning at 7:19 pm; axial cross-sectional rapid acquisition with relaxation enhancement (RARE) images were taken with field of view (FOV) = $45 \times 45 mm^2$, 300×300 pixels, slice thickness = 1 mm; 1 cm scale bar.

observed, and the abdominal cavity bent inwards. No residual oocytes were visible in MR images. The females lost 38.3–45.3% of their body weight in oocyte mass.

4 | DISCUSSION

4.1 | MRI methods

Many studies have demonstrated the suitability of MRI for estimating organ volume or studying the anatomy of live[16,46,47] and preserved marine specimens.[15,48] In most in vivo MRI studies, animals are anaesthetised to avoid movement artefacts and to increase possible measuring time and thus improve image quality.[22,49] In the present study, we optimised imaging parameters and acquisition time, to apply MRI for longitudinal studies on the development of unanaesthetised and unrestrained fish. Measuring without anaesthesia is preferable in ectothermic animals such as fish to prevent the anaesthesia from altering the physiological parameters. Several anaesthetics that are applied for fish can have long-lasting effects on physiological parameters such as blood chemistry, heart rate or respiration (reviewed in previous works[50–52]).

In general, the MR imaging sequence and parameters used depend on the properties, T1 and T2 values of the tissue of interest. The selected TE, TR values and flip angle (in case of FcFLASH) were based on the comparison of the contrast between the gonads and the surrounding tissue and limitation in acquisition time per scan (to avoid potential movement of fish). Here, we used two different imaging techniques, RARE and FcFLASH, which both produced good morphological results, particularly for the gonads and its surrounding tissue. However, in the gradient echo T1-weighted images (FcFLASH), susceptibility artefacts were caused by the gas-filled swim bladder leading to signal extinction of the surrounding tissue including the gonad, whereas the spin echo T2-weighted images (RARE) showed a clearer separation with lesser signal extinctions around the swim bladder. Similar observations have been made for in vivo imaging of Atlantic cod (*Gadus morhua* Linnaeus, 1758)[46] and for in vivo imaging of the brain in zebrafish (*D. rerio*).[21] In RARE images, the seawater signal is cancelled out due to flow effects and appears dark. The non-laminar flow in the animal chamber caused by the fish and its movement is leading to inhomogeneous signal dropouts. The seawater signal was further suppressed by saturation slices but only achieved inhomogeneous FOV saturation due to the flow.

Bock et al.[26] could show a strong correlation between body weight and MRI body volume in preserved samples of the Antarctic silverfish, *Pleuragramma antarctica* (Boulenger, 1902). In the present study, the ratio of calculated gonad volume to measured gonad weight was approximately 1 in males and females. This is also reflected in similar GSIs calculated based on weight or volume and confirms that the MRI method is a suitable alternative for determining organ volumes including gonads without sacrificing the fish. The weight-to-volume ratio in ovaries and the GSI compared with GSI $_{VG}$ appear to correlate better compared to testes. This difference could be attributed to different densities of male and female gonads. The spawned eggs are buoyant in seawater and have a density of 1.022–1.024 g cm^{-3}, as reported by Spencer et al.,[53] resulting in a ratio of close to 1. The weaker weight:volume correlation in the testis and overestimation in GSI $_{VG}$ compared with GSI might be caused by a higher variation in MRI volume data, which can be explained by two related reasons. First, it is more difficult to analyse male MRI data due to the less pronounced structure of the testis in comparison with the surrounding tissue, and thus, MRI-based testis volume could be more prone to errors. Second, gonad weight might be underestimated due to the loss of sperm during dissection of testis. A larger replica number would help to minimise this error and most likely improve the correlation. However, other studies found comparable volume:weight relationships for estimated gonad volume based on MRI techniques in starfish,[49] oyster[54,55] and ovary of anaesthetised *R. ventralis*, a cyprinid fish species.[23]

In general, the MRI approach resulted in reliable gonad volume data and may be a major improvement in reducing the number of experimental animals. Studies employing classical, ecological indices such as GSI or histology to assess maturation status typically use 5–10 specimens per group and sampling time points.[1,6,56] A comparable experimental design without repeated measurements would therefore require a total sample size of 30–60 fish (scarifying 5–10 male and female polar cod per month from December to February), which demonstrates that we were able to reduce the number of animals by three to six-fold. A study investigating the seasonal gonad development and energy investment of polar cod from December to February sacrificed 52 fish,[1] whereas another study investigating the effect of dietary crude oil exposure on reproduction sampled a total of 249 polar cod (four treatments and five time points) from June to January.[6] Despite the high number of individuals sacrificed in these studies, an unbalanced sex ratio was found in both studies. This highlights the necessity for a tool to identify the sex non-invasively and reduce the sample size further.

Even though it is a non-invasive approach, the effect of repeated handling such as weight loss or spontaneous spawning needs to be considered. Van den Thillart et al.[57] suggested a phosphocreatine/inorganic phosphate (PCr/Pi) ratio of about 15 using in vivo 31P-NMR spectroscopy as an indicator for low stressed fish inside a magnet, which was confirmed by several other fish species later on such as (crucian carp (*Carassius carassius* Linnaeus, 1758) and common carp (*Cyprinus carpio* Linnaeus, 1758),[25] Antarctic eelpout (*Pachycara brachycephalum* Pappenheim, 1912) and North Sea eelpout (*Zoarces viviparus* Linnaeus, 1758),[17] Atlantic cod.[58] However, it cannot be excluded whether females are not influenced by the measurements in the MR scanner at the end of the developmental phase of the gonads, as in our study, some females spontaneously spawned in the late stage of gonadal development. Indeed, a study on oxygen consumption of polar cod exposed to dietary crude oil reported weight loss partially attributed to the effects of repeated handling.[8] Thus, the potential effects of repeated MRI measurements on fish should be further investigated by monitoring the, for example PCr/Pi ratio and body weight over the monitoring period.

4.2 | Reproduction and gonad development of polar cod

The sex of polar cod cannot be distinguished externally.[35,40,59] Females tend to grow larger than males over their life span.[35] This size difference however cannot be easily distinguished from age-related growth that complicates a balanced sex ratio in wild-caught animals. *B. saida* has been used to develop an in vivo method to distinguish between males and females and visualise gonads in a longitudinal MRI study. In comparison with previous studies on polar cod,[1,2] we were able to follow individual gonad development in vivo over a period of 4 months. From November 2021 onwards, the gonads were clearly visible in all observed *B. saida*. The onset of gonad maturation of *B. saida* starts around August to September. Initial method adjustments prevented us from starting our monitoring at the very beginning of the maturation phase that would be interesting for future studies.

Polar cod show sex-specific differences in gonad maturation (reproductive strategies), and the male gonads reached maximum size already in November, whereas the female gonads reached full size in February.[1,35] This pattern is reflected by minor changes in male gonad volume and a

significant increase in female gonad volume throughout this study. The average volume-based GSI $_{VG}$ of 20.3 ± 1.8% for males was lower than the range of 30–35% reported in previous studies for males, whereas the average volume-based GSI $_{VG}$ of 46.5 ± 0.9% for females was consistent with values of 21–48% found in previous studies for February.[1,6] The difference in our GSI $_{VG}$ and the literature values in males could be related to the weaker correlation of MRI-based gonad volume and gonad weight found in this study. Mean male gonad volume changed little during the monitoring period, but two males (M1 and M2) showed a decrease in gonad volume in January. Whether the decrease in gonad volume in January is caused by an earlier release of sperm or technical reasons remains unclear. This may call for further method improvement to control the exact FOV or contrast optimisation in future studies. The image contrast of male gonads changed from a light grey to a heterogeneous lighter grey in February, and this might be related to the formation of spermatozoa, the final stage of sperm development. In Atlantic cod, spermatogenesis (the formation of spermatozoa) occurs at different times in different regions of the testis, starting in the cells closest to the centre of the testis.[56] This could be a possible explanation for the heterogeneous contrast observed in the gonads of two males (M1 and M3).

Gonads of female *B. saida* grow exponentially in the last 2 months prior to spawning and mature gonads reach a water content of around 90%.[1] The high-water content of female mature gonads may explain the high contrast observed at the late stage, as the MR contrast is based on water content and biochemical properties of the tissue. The increase in gonad volume was caused by an increase in oocyte volume, which was confirmed by a strong correlation of gonad and oocyte volume. The female with the largest oocytes also reached the largest gonad volume in January. In addition, females appeared gravid and could be identified as close to spawning by visual inspection due to an enlarged abdominal cavity.[60] These findings agree with a previous study that showed a significant increase in oocyte diameter mirrored by an increase in GSI for *B. saida* from November to January.[2] The highest variability in oocyte diameter among females with a range of 705–1164 μm ($n = 5$) was found in January. This was accompanied by a higher contrast of oocytes starting at an oocyte size of around 928 μm, potentially the onset of hydration of oocytes and final maturation. The final maturation stage is characterised by the first meiotic division and a hydration phase leading to a massive water influx in oocytes,[36,61,62] which would induce a higher MRI signal with the used acquisition parameters (higher water content). For Atlantic cod, final maturation of oocytes was observed at a size of around 940 μm and associated with high water uptake prior to ovulation (Kjesbu et al.[63] and reference therein). Nahrgang et al.[2] reported a size of 600 μm for oocytes in a histological study in *B. saida* from the archipelago of Svalbard (Norway), and no hydrated oocytes were found suggesting that polar cod had not yet reached the final maturation in January. In the female displaying an intermediate stage, a difference in size was found between the dark and grey oocytes (790 and 1020 μm, respectively). In polar cod, the final maturation of oocytes lasts around 1 week.[2,64] This could be a reason why we observed the intermediate state of differently coloured oocytes only in one female. In future studies, shorter measuring intervals during the final maturation phase might catch the onset of hydration of oocytes and confirm our interpretation.

The mean oocyte diameter of 1.35 mm in February is smaller than the egg size of 1.5–1.9 mm found in previous studies for *B. saida* shortly before spawning.[39,40,60,65] The smaller oocyte diameter might be caused by the fact that the oocyte diameter was measured inside the gonads, where the oocytes are densely packed and compressed by surrounding tissue. The size difference could also be attributed to perivitelline space, which is formed by water influx after eggs are spawned.[62,65] Even though the oocyte diameter was slightly smaller, the total number of eggs (16,700–29,700 eggs per female) is within the range reported in literature, supporting that the assumption of spherical shape without interspace of connective tissue between oocytes is a valid approximation. The estimates of eggs produced per female given in the literature vary between 13,000 and 75,000, depending on the region, age and size of the female.[1,35,59,66] Polar cod is a total synchronous spawner releasing all eggs in a single spawning event, and few to no eggs are found in the gonads after spawning.[2,40,60] Females can lose up to 50% of their body weight as egg mass,[1] which is only slightly higher than the estimated weight loss of 38–45% found in this study. With the use of MR imaging, we were able to document the severe changes in female gonads after spawning and support the hypothesis of polar cod being a total synchronous spawner, with one exception observed for the F1 female in February.

5 | CONCLUSION

In this study, we demonstrated that MRI techniques can be used to monitor gonad development in unrestrained fish with high resolution. These methods significantly reduce the number of animals needed for long-term experiments compared with a similar experiment without repeated sampling as they allow for monitoring individuals continuously instead of frequent sub-sampling events. This plays a major role in the application of the 3R rules (replace, reduce and refine) and to optimise the use of non-model species that are difficult to access due to remote locations. This non-invasive approach is easily transferable to other species and has great potential for various applications, for example for ecological and aquaculture research such as monitoring gonad development and reproductive features over time under normal conditions or in response to environmental stressors.

marine life: from genes to ecosystems, of the Alfred Wegener Institute Helmholtz Centre for Polar and Marine Research, Germany. The authors thank the three reviewers for their valuable comments. Open Access funding enabled and organized by Projekt DEAL.

CONFLICT OF INTEREST STATEMENT

The authors declare that they have no conflict of interest.

DATA AVAILABILITY STATEMENT

The data will be made available on the data repository PANGEA.

ORCID

Nicole Vogt https://orcid.org/0000-0003-2996-6899
Felizitas C. Wermter https://orcid.org/0000-0002-7933-8447
Jasmine Nahrgang https://orcid.org/0000-0002-4202-5922
Daniela Storch https://orcid.org/0000-0003-3090-7554
Christian Bock https://orcid.org/0000-0003-0052-3090

REFERENCES

1. Hop H, Graham M, Trudeau VL. Spawning energetics of Arctic cod (*Boreogadus saida*) in relation to seasonal development of the ovary and plasma sex steroid levels. *Can J Fish Aquat Sci*. 1995;52(3):541-550. doi:10.1139/f95-055
2. Nahrgang J, Storhaug E, Murzina SA, Delmas O, Nemova NN, Berge J. Aspects of reproductive biology of wild-caught polar cod (*Boreogadus saida*) from Svalbard waters. *Polar Biol*. 2016;39(6):1155-1164. doi:10.1007/s00300-015-1837-2
3. Lahnsteiner F, Lahnsteiner E, Kletzl M. Age and species related differences in gonad development of triploid Salmonidae. *J Appl Aquac*. 2021;33(3):183-208. doi:10.1080/10454438.2020.1760993
4. Mazzeo I, Peñaranda DS, Gallego V, et al. Temperature modulates the progression of vitellogenesis in the European eel. *Aquaculture*. 2014;434:38-47. doi:10.1016/j.aquaculture.2014.07.020
5. Vitale F, Cardinale M, Svedäng H. Evaluation of the temporal development of the ovaries inGadus morhuafrom the sound and Kattegat, North Sea. *J Fish Biol*. 2005;67(3):669-683. doi:10.1111/j.0022-1112.2005.00767.x
6. Bender ML, Frantzen M, Vieweg I, et al. Effects of chronic dietary petroleum exposure on reproductive development in polar cod (*Boreogadus saida*). *Aquat Toxicol*. 2016;180:196-208. doi:10.1016/j.aquatox.2016.10.005
7. Strople LC, Vieweg I, Yadetie F, et al. Spawning time in adult polar cod (*Boreogadus saida*) altered by crude oil exposure, independent of food availability. *J Toxicol Environ Health a*. 2023;1-24. doi:10.1080/15287394.2023.2228535
8. Nahrgang J, Bender ML, Meier S, Nechev J, Berge J, Frantzen M. Growth and metabolism of adult polar cod (*Boreogadus saida*) in response to dietary crude oil. *Ecotoxicol Environ Saf*. 2019;180:53-62. doi:10.1016/j.ecoenv.2019.04.082
9. Russell WMS, Burch RL. *The principles of humane experimental technique*. Methuen & Co Ltd; 1959.
10. Hubrecht C. The 3Rs and humane experimental technique: implementing change. *Animals*. 2019;9(10):754. doi:10.3390/ani9100754
11. Clear E, Grant RA, Carroll M, Brassey CA. A review and case study of 3D imaging modalities for female Amniote reproductive anatomy. *Integr Comp Biol*. 2022;62(3):542-558. doi:10.1093/icb/icac027
12. Karlsen R, Holm JC. Ultrasonography, a non–invasive method for sex determination in cod (*Gadus morhua*). *J Fish Biol*. 1994;44(6):965-971. doi:10.1111/j.1095-8649.1994.tb01268.x
13. Bureau du Colombier S, Jacobs L, Gesset C, Elie P, Lambert P. Ultrasonography as a non-invasive tool for sex determination and maturation monitoring in silver eels. *Fish Res*. 2015;164:50-58. doi:10.1016/j.fishres.2014.10.015
14. Ledoré Y, Bestin A, Haffray P, et al. Sex identification in immature Eurasian perch (*Perca fluviatilis*) using ultrasonography. *Aquacult Res*. 2021;52(12):6046-6051. doi:10.1111/are.15465
15. Ziegler A, Kunth M, Mueller S, et al. Application of magnetic resonance imaging in zoology. *Zoomorphology*. 2011;130(4):227-254. doi:10.1007/s00435-011-0138-8
16. Blackband SJ, Stoskopf MK. In vivo nuclear magnetic resonance imaging and spectroscopy of aquatic organisms. *Magn Reson Imaging*. 1990;8(2):191-198. doi:10.1016/0730-725X(90)90253-X
17. Bock C, Sartoris FJ, Wittig RM, Pörtner HO. Temperature-dependent pH regulation in stenothermal Antarctic and eurythermal temperate eelpout (Zoarcidae): an in-vivo NMR study. *Polar Biol*. 2001;24(11):869-874. doi:10.1007/s003000100298
18. Wu JL, Zhang JL, Du XX, et al. Evaluation of the distribution of adipose tissues in fish using magnetic resonance imaging (MRI). *Aquaculture*. 2015;448:112-122. doi:10.1016/j.aquaculture.2015.06.002
19. Toussaint C, Fauconneau B, Médale F, et al. Description of the heterogeneity of lipid distribution in the flesh of brown trout (*Salmo trutta*) by MR imaging. *Aquaculture*. 2005;243(1–4):255-267. doi:10.1016/j.aquaculture.2004.09.029
20. Kabli S, He S, Spaink HP, et al. *In vivo* magnetic resonance imaging to detect malignant melanoma in adult zebrafish. *Zebrafish*. 2010;7(2):143-148. doi:10.1089/zeb.2009.0649
21. Merrifield GD, Mullin J, Gallagher L, et al. Rapid and recoverable in vivo magnetic resonance imaging of the adult zebrafish at 7T. *Magn Reson Imaging*. 2017;37:9-15. doi:10.1016/j.mri.2016.10.013
22. Hamilton N, Allen C, Reynolds S. Longitudinal MRI brain studies in live adult zebrafish. *NMR Biomed*. 2023;36(7):e4891. doi:10.1002/nbm.4891
23. Pan L, Hu J, Peng C, et al. Use of magnetic resonance imaging to assess ovarian maturation in live *Rhinogobio ventralis* (Sauvage & Dabry de Thiersant, 1874). *Theriogenology*. 2016;86(8):1969-1974. doi:10.1016/j.theriogenology.2016.06.015

24. Kaneko G, Ushio H, Ji H. Application of magnetic resonance technologies in aquatic biology and seafood science. *Fish Sci*. 2019;85(1):1-17. doi:10.1007/s12562-018-1266-6

25. van der Linden A, Verhoye M, Pörtner HO, Bock C. The strengths of *in vivo* magnetic resonance imaging (MRI) to study environmental adaptational physiology in fish. *Magn Reson Mater Phys Biol Med*. 2004;17(3–6):236-248. doi:10.1007/s10334-004-0078-0

26. Bock C, Wermter FC, Mintenbeck K. MRI and MRS on preserved samples as a tool in fish ecology. *Magn Reson Imaging*. 2017;38:39-46. doi:10.1016/j.mri.2016.12.017

27. Maus B, Pörtner HO, Bock C. Studying the cardiovascular system of a marine crustacean with magnetic resonance imaging at 9.4 T. *Magn Reson Mater Phys Biol Med*. 2019;32(5):567-579. doi:10.1007/s10334-019-00752-4

28. Pörtner HO, Farrell AP. Physiology and climate change. *Science*. 2008;322(5902):690-692. doi:10.1126/science.1163156

29. Kunz KL, Frickenhaus S, Hardenberg S, et al. New encounters in Arctic waters: a comparison of metabolism and performance of polar cod (*Boreogadus saida*) and Atlantic cod (*Gadus morhua*) under ocean acidification and warming. *Polar Biol*. 2016;39(6):1137-1153. doi:10.1007/s00300-016-1932-z

30. Moreira JM, Mendes AC, Maulvault AL, et al. Impacts of ocean warming and acidification on the energy budget of three commercially important fish species. *Conserv Physiol*. 2022;10(1):coac048. doi:10.1093/conphys/coac048

31. Mecklenburg CW, Møller PR, Steinke D. Biodiversity of arctic marine fishes: taxonomy and zoogeography. *Mar Biodivers*. 2011;41(1):109-140. doi:10.1007/s12526-010-0070-z

32. Bradstreet MSW. Occurrence, habitat use, and behavior of seabirds, marine mammals, and Arctic cod at the pond inlet ice edge. *Arctic* 1982;35(1):28–40. Accessed January 29, 2024. https://www.jstor.org/stable/40509300, doi:10.14430/arctic2305

33. Bradstreet MSW, Finley KJ, Sekerak AD, et al. Aspects of the biology of Arctic cod (*Boreogadus saida*) and its importance in arctic marine food chains. *Can Tech Rep Fish Aquat Sci*. 1986;1491:1-139. doi:10.46292/sci21-00096

34. Mueter FJ, Nahrgang J, John Nelson R, Berge J. The ecology of gadid fishes in the circumpolar Arctic with a special emphasis on the polar cod (*Boreogadus saida*). *Polar Biol*. 2016;39(6):961-967. doi:10.1007/s00300-016-1965-3

35. Nahrgang J, Varpe Ø, Korshunova E, et al. Gender specific reproductive strategies of an arctic key species (*Boreogadus saida*) and implications of climate change. *PLoS ONE*. 2014;9(5):e98452. doi:10.1371/journal.pone.0098452

36. Murua H, Saborido-Rey F. Female reproductive strategies of marine fish species of the North Atlantic. *J Northwest Atl Fish Sci*. 2003;33:23-31. doi:10.2960/J.v33.a2

37. Craig PC, Griffiths WB, Haldorson L, McElderry H. Ecological studies of Arctic cod (*Boreogadus saida*) in Beaufort Sea coastal waters, Alaska. *Can J Fish Aquat Sci*. 1982;39(3):395-406. doi:10.1139/f82-057

38. Hop H, Gjøsæter H. Polar cod (*Boreogadus saida*) and capelin (*Mallotus villosus*) as key species in marine food webs of the Arctic and the Barents Sea. *Mar Biol Res*. 2013;9(9):878-894. doi:10.1080/17451000.2013.775458

39. Rass TS. Spawning and development of polar cod. Rapports et Procès-Verbeaux des Réunions Conseil International l''Exploration de la Mer. 1968;158:135–137. Accessed December 5, 2023. 10.17895/ices.pub.19275401

40. Graham M, Hop H. Aspects of reproduction and larval biology of Arctic cod (*Boreogadus saida*). *Arctic*. 1995;48(2):130-135. doi:10.14430/arctic1234

41. Wermter FC, Maus B, Pörtner H, Dreher W, Bock C. CO_2 induced pH_i changes in the brain of polar fish: a TauCEST application. *NMR Biomed*. 2018; 31(8):e3955. doi:10.1002/nbm.3955

42. R Core Team. R: A language and environment for statistical computing. Published online 2023. https://www.R-project.org/

43. Neuwirth E. RColorBrewer: ColorBrewer Palettes. Published online 2022. https://CRAN.R-project.org/package=RColorBrewer

44. Pinheiro J, Bates D. nlme: linear and nonlinear mixed effects models. Published online 2023. https://CRAN.R-project.org/package=nlme

45. Pinheiro J, Bates D. *Mixed-effects models in S and S-PLUS*. Springer-Verlag; 2000. doi:10.1007/b98882

46. Bock C, Sartoris FJ, Pörtner HO. *In vivo* MR spectroscopy and MR imaging on non-anaesthetized marine fish: techniques and first results. *Magn Reson Imaging*. 2002;20(2):165-172. doi:10.1016/S0730-725X(02)00482-4

47. Clark JR, Camus AC, Comolli J, Divers SJ, Gendron KP. MRI of the live fish brain at 3 tesla: feasibility, technique and interspecies anatomic variations. *Vet Radiol Ultrasound*. 2023;64(1):75-85. doi:10.1111/vru.13128

48. Kline TL, Sussman CR, Irazabal MV, et al. Three-dimensional NMR microscopy of zebrafish specimens. *NMR Biomed*. 2019;32(1):e4031. doi:10.1002/nbm.4031

49. Sigl R, Imhof H, Settles M, Laforsch C. A novel, non-invasive and in vivo approach to determine morphometric data in starfish. *J Exp Mar Biol Ecol*. 2013;449:1-9. doi:10.1016/j.jembe.2013.08.002

50. Topic Popovic N, Strunjak-Perovic I, Coz-Rakovac R, et al. Tricaine methane-sulfonate (MS-222) application in fish anaesthesia. *J Appl Ichthyol*. 2012; 28(4):553-564. doi:10.1111/j.1439-0426.2012.01950.x

51. Martins T, Valentim A, Pereira N, Antunes LM. Anaesthetics and analgesics used in adult fish for research: a review. *Lab Anim*. 2019;53(4):325-341. doi:10.1177/0023677218815199

52. Soldatov AA. Functional effects of the use of anesthetics on Teleostean fishes (review). *Inland Water Biol*. 2021;14(1):67-77. doi:10.1134/S1995082920060139

53. Spencer ML, Vestfals CD, Mueter FJ, Laurel BJ. Ontogenetic changes in the buoyancy and salinity tolerance of eggs and larvae of polar cod (*Boreogadus saida*) and other gadids. *Polar Biol*. 2020;43(8):1141-1158. doi:10.1007/s00300-020-02620-7

54. Flahauw E, Quellec S, Davenel A, Degremont L, Lapegue S, Hatt PJ. Gonad volume assessment in the oyster *Crassostrea gigas*: comparison between a histological method and a magnetic resonance imaging (MRI) method. *Aquaculture*. 2012;370:84-89. doi:10.1016/j.aquaculture.2012.10.008

55. Davenel A, Quellec S, Pouvreau S. Noninvasive characterization of gonad maturation and determination of the sex of Pacific oysters by MRI. *Magn Reson Imaging*. 2006;24(8):1103-1110. doi:10.1016/j.mri.2006.04.014

56. Almeida FFL, Kristoffersen C, Taranger GL, Schulz RW. Spermatogenesis in Atlantic cod (*Gadus morhua*): a novel model of cystic germ cell development. *Biol Reprod*. 2008;78(1):27-34. doi:10.1095/biolreprod.107.063669

57. van den Thillart G, Körner F, van Waarde A, Erkelens C, Lugtenburg J. A flow-through probe for in vivo 31P NMR spectroscopy of unanesthetized aquatic vertebrates at 9.4 tesla. *J Magn Reson (1969)*. 1989;84(3):573-579. doi:10.1016/0022-2364(89)90121-2

58. Sartoris FJ, Bock C, Serendero I, Lannig G, Pörtner HO. Temperature-dependent changes in energy metabolism, intracellular pH and blood oxygen tension in the Atlantic cod. *J Fish Biol*. 2003;62(6):1239-1253. doi:10.1046/j.1095-8649.2003.00099.x

59. Kent D, Drost HE, Fisher J, Oyama T, Farrell AP. Laboratory rearing of wild Arctic cod *Boreogadus saida* from egg to adulthood. *J Fish Biol*. 2016;88(3): 1241-1248. doi:10.1111/jfb.12893

60. Sakurai Y, Ishii K, Nakatani T, Yamaguchi H, Anma G, Jin M. Reproductive characteristics and effects of temperature and salinity on the development and survival of eggs and larvae of Arctic cod (*Boreogadus saida*). *Memoirs Fac Fish Hokkaido Univ*. 1998;45(1):77-89.

61. Lubzens E, Young G, Bobe J, Cerdà J. Oogenesis in teleosts: how fish eggs are formed. *Gen Comp Endocrinol*. 2010;165(3):367-389. doi:10.1016/j.ygcen.2009.05.022

62. Craik JCA, Harvey SM. The causes of buoyancy in eggs of marine teleosts. *J Mar Biol Assoc UK*. 1987;67(1):169-182. doi:10.1017/S0025315400026436

63. Kjesbu OS, Kryvi H, Sundby S, Solemdal P. Buoyancy variations in eggs of Atlantic cod (*Gadus morhua* L.) in relation to chorion thickness and egg size: theory and observations. *J Fish Biol*. 1992;41(4):581-599. doi:10.1111/j.1095-8649.1992.tb02685.x

64. Christophorov OL. Gametogenesis and reproduction cycle of polar cod *Boreogadus saida* (Lepechin) in the Barents Sea. *VNIRO Proc*. 1978;130:33-46.

65. Aronovich TM, Doroshev SI, Spectorova LV, Makhotin VM. Egg incubation and larval rearing of navaga (*Eleginus navaga* pall.), polar cod (*Boreogadus saida* lepechin) and arctic flounder (*Liopsetta glacialis* pall.) in the laboratory. *Aquaculture*. 1975;6(3):233-242. doi:10.1016/0044-8486(75)90043-5

66. Aune M, Raskhozheva E, Andrade H, et al. Distribution and ecology of polar cod (*Boreogadus saida*) in the eastern Barents Sea: a review of historical literature. *Mar Environ Res*. 2021;166:105262. doi:10.1016/j.marenvres.2021.105262